

promoting access to White Rose research papers



Universities of Leeds, Sheffield and York
<http://eprints.whiterose.ac.uk/>

This is an author produced version of a paper published in **Journal of Composites for Construction**.

White Rose Research Online URL for this paper:

<http://eprints.whiterose.ac.uk/78009>

Published paper

Garcia, R., Jemaa, Y., Helal, Y., Guadagnini, M. and Pilakoutas, K. (2013)
Seismic strengthening of severely damaged beam-column RC joints using CFRP.
Journal of Composites for Construction, 18 (2). ISSN 1090-0268

[http://dx.doi.org/10.1061/\(ASCE\)CC.1943-5614.0000448](http://dx.doi.org/10.1061/(ASCE)CC.1943-5614.0000448)

White Rose Research Online
eprints@whiterose.ac.uk

21 **Introduction**

22 Recent strong earthquakes in developing countries (Kashmir, 2005; China, 2008; Indonesia, 2009 and Haiti,
23 2010) caused extensive economic and human losses due to the poor behavior of many old reinforced concrete
24 (RC) buildings. Many structural failures in these structures can be attributed to the lack of internal steel
25 stirrups in beam-column joints, which increase the seismic vulnerability of the building. The local
26 strengthening of these deficient elements is a feasible option for reducing the vulnerability of such
27 substandard buildings. Over the last twenty years, externally bonded Fiber Reinforced Polymers (FRP) have
28 been used extensively to strengthen seismically deficient elements. In comparison to other strengthening
29 materials, FRP possess advantages such as high resistance to corrosion, excellent durability, high strength to
30 weight ratio, adaptability to different shapes, and ease and speed of in-situ application (Gdoutos et al. 2000).

31 Numerous experimental studies have demonstrated the effectiveness of FRP strengthening at improving the
32 seismic behavior of substandard RC beam-column joints (e.g. Mosallam 2000; Gergely et al. 2000; Granata
33 and Parvin 2001; El-Amoury and Ghobarah 2002; Antonopoulos and Triantafillou 2003; Prota 2004; Said
34 and Nehdi 2004; Ghobarah and El-Amoury 2005; Mukherjee and Joshi 2005; Engindeniz 2008; Pantelides
35 2008; Akguzel and Pampanin 2010; Alsayed et al. 2010; Le-Trung et al. 2010; Boussselham, 2010; Parvin et
36 al. 2010; Al-Salloum 2011a; 2011b; Ilki et al. 2011). Most of these studies aimed at a) assessing the
37 effectiveness of FRP at preventing premature shear failure of joints without internal confinement, and b)
38 changing the strength hierarchy of the joints to promote yielding in the beam reinforcement. Despite the
39 extensive research, the majority of these studies focused on undamaged specimens, whilst less research has
40 investigated the use of FRP as a post-earthquake strengthening solution in joints that experienced severe
41 damage. Different rehabilitation techniques have been used to repair damaged joints, including a) crack
42 injection with epoxy resin and partial core replacement with high-strength cement paste or mortar
43 (Karayannis et al. 1998; Karayannis and Sirkelis 2008; Sasmal et al. 2011), b) complete core replacement
44 with new concrete (Ghobarah and Said 2001; 2002), and c) partial core replacement with high-strength
45 mortar (Tsonos 2008; Sezen 2012). However, researchers rarely attempted to evaluate the individual
46 contributions of the repairing technique and the FRP strengthening to the total strength of the joint. As shown

47 by Karayannis et al. (1998), the use of high-strength materials in the rehabilitation can by itself enhance the
48 strength of the joint considerably. Crack injection and mortar repairing have proven effective at low to
49 moderate levels of damage, but they may be less effective when severe damage occurs (e.g. complete
50 concrete crushing in the core) or bond between reinforcing bars and concrete is lost. In this case, the complete
51 replacement of the core with new concrete may be necessary to recover its structural integrity before applying
52 the FRP. Nonetheless, results of joints rehabilitated and strengthened with this solution are not available in
53 the literature. A combination of core replacement with high-strength concrete and FRP strengthening can be
54 suitable for rehabilitating existing substandard buildings in developing countries, where strengthening
55 interventions are usually carried out in structures damaged after an earthquake.

56 This study is part of the multistage EU-funded project BANDIT (SERIES Program FP7) which focuses on
57 the seismic strengthening of substandard RC structures typical of developing countries. The work carried out
58 under this project comprises tests on beam-column joints and shake table tests on a full-scale RC building
59 (Garcia 2013; Garcia et al. 2014a). This paper focuses on the former tests and investigates the seismic
60 behavior of severely damaged full-scale RC beam-column joints rehabilitated and strengthened with
61 externally bonded CFRP. The geometry and detailing of the tested specimens were similar to those used in
62 the joints of the BANDIT building (Garcia et al. 2014a). Therefore, the current tests aimed at i) assessing the
63 capacity and behavior of substandard joints under severe demands, and ii) investigating effective
64 rehabilitation and strengthening solutions for damaged joints with FRP sheets. The experimental results are
65 discussed and compared to predictions obtained according to existing models.

66 **Experimental program**

67 Three RC beam-column joints were tested in two successive phases. In phase 1, the bare joints were
68 subjected to cyclic tests up to drifts of about 4.0%, and the tests were halted when the peak capacity dropped
69 by 50%. As these tests produced severe damage in the joint core, the damaged concrete was fully removed
70 and replaced with new high-strength concrete. The specimens were subsequently strengthened with externally
71 bonded FRP sheets and retested up to failure (phase 2).

72 **Geometry of specimens**

73 The specimens simulated a full-scale 2D exterior joint between contra-flexure points of a floor in a multi-
74 story moment-resisting frame, but excluding the slabs (see Fig. 1(a)). The column had a cross section of
75 260×260 mm and a height of 2700 mm. The longitudinal column reinforcement consisted of 16 mm bars (see
76 Fig. 1(b)). These bars were lapped over a length $l_b=25d_b$ (d_b = bar diameter) just above the joint core to
77 represent typical construction practices of developing countries.

78 The beam had a cross section of 260×400 mm and a length of 1650 mm. The main flexural reinforcement
79 consisted of 16 mm bars as shown in Fig. 1(b). Three types of anchorage detailing were examined for the top
80 beam reinforcement as shown in Fig. 1(c). To study the effect of deficient bar anchorage, the bottom beam
81 reinforcement of detailing types A and B was anchored into the joint for a length of 220 mm only
82 (approximately $14d_b$), with no hooks or bends. This short anchorage length would be deemed insufficient to
83 develop the full capacity of the 16 mm bars according to current design recommendations. The column-to-
84 beam relative flexural strength ratio ($\Sigma M_{Rcol}/\Sigma M_{Rbeam}$) of the specimens was approximately 1.0, and therefore
85 the strong column-weak beam strength hierarchy intended by current design philosophy was not satisfied.
86 Moreover, the specimens were designed to fail at the core where no confining stirrups were provided. To
87 prevent a shear failure outside the joint core, the column and beam were reinforced with 8 mm transverse
88 stirrups spaced at 150 mm centers. The stirrups were closed with 90° hooks instead of 135° hooks typically
89 required by current seismic codes.

90 Table 1 gives some of the main characteristics of the beam-column joints including concrete strength. The
91 specimens are identified using an ID code in which the first letter stands for “Joint” and the second for the
92 type of beam reinforcement detailing (A, B or C), respectively. The letters after the number indicates the
93 condition of the joints during the test: “R” stands for a joint tested in rehabilitated condition (i.e., with a new
94 concrete core), whilst “RF” stands for a joint tested in rehabilitated condition and strengthened with FRP
95 sheets. The core of joint JB2RF was recast again and the specimen (renamed as JB2R) was retested to
96 examine the effect of core replacement on the joint shear strength.

97 **Material properties**

98 The joints were cast using two batches of ready mixed concrete. A steel roller was inserted at the center of the
99 cross section of the beam tip during casting, as shown in Fig. 1(a). Following casting, the specimens were
100 cured for seven days in the formwork and then stored under standard laboratory conditions. The mean
101 concrete compressive strength (f_{cm}) was determined from tests on three 150×300 mm concrete cylinders
102 according to BS EN 12390-3 (BSI 2009a). The indirect tensile splitting strength (f_{ctm}) was obtained from tests
103 on three 100×200 mm cylinders according to BS EN 12390-6 (BSI 2009b). All cylinders were cast at the
104 same time and cured together with the joints. Table 1 summarizes the mean values and standard deviations
105 obtained from the tests.

106 Grade S500 ribbed bars were used as reinforcement for all joints. The yield and tensile strengths of the steel
107 reinforcement were obtained from three test samples and were found to be $f_y=612$ MPa and $f_u=726$ MPa for
108 the 8 mm bar, and $f_y=551$ MPa and $f_u=683$ MPa for the 16 mm bar, respectively. The elastic modulus of both
109 bars was determined as $E_s=209$ GPa.

110 After phase 1 of testing, the damaged concrete in the core of the joints was completely removed and replaced
111 with new highly flowable concrete. In joint JB2, the bottom bars of the beam were welded to the 90° bends of
112 the top beam reinforcement as shown in Fig. 1(d) (JB2RF and JB2R in phase 2). Before casting the new
113 concrete, the contact surfaces of the existing concrete were thoroughly cleaned with compressed air and
114 moistened for 24 hours. No bonding agent was used between the new and existing concrete. At the end of
115 casting, the new core was cured in the mold for three days, and without the mold for four additional days.

116 Following the core replacement, the joints were strengthened with externally bonded CFRP using a wet lay-
117 up procedure. The unidirectional CFRP sheets had the following nominal properties provided by the
118 manufacturer: tensile strength $f_f=4140$ MPa, elastic modulus $E_f=241$ GPa, ultimate elongation $\varepsilon_{fu}=1.70\%$, and
119 sheet thickness $t_f=0.185$ mm. Before bonding the CFRP sheets, the concrete surfaces were wire brushed and
120 cleaned with pressurized air to improve adherence, and the corners were rounded off to a radius of
121 approximately 15 mm.

122 **Experimental setup and instrumentation**

123 The joints were tested with the column in horizontal position as shown in Fig. 2. A guiding device consisting
124 of an oiled roller inserted between two parallel steel plates was used at the beam tip to restrain possible out-
125 of-plane movement at large displacements, but such device allowed free displacement and rotation of the
126 beam in the direction of testing. Displacements were monitored using Linear Variable Differential
127 Transformers (LVDTs) at the locations shown in Fig. 2. Deformations of the joint core were also measured
128 using a set of 16 linear potentiometers. The strain developed along the beam and column steel reinforcement
129 and CFRP sheets was monitored using strategically placed foil-type electrical resistance strain gages (see Fig.
130 3(a)).

131 The cyclic load was applied to the beam in displacement control using a servo-hydraulic actuator (see Fig. 2).
132 Three push-pull cycles were applied at drift ratios δ (δ =beam tip displacement/beam length) of $\pm 0.25\%$,
133 $\pm 0.5\%$, $\pm 0.75\%$, $\pm 1.0\%$, $\pm 1.5\%$, $\pm 2.0\%$, $\pm 3.0\%$, $\pm 4.0\%$ and $\pm 5.0\%$. Cycles at $\delta \pm 0.75\%$ and $\pm 1.5\%$ were not
134 applied in phase 2 to reduce the testing time. Each cycle was applied in the push (+) direction first, which
135 tensioned the top beam reinforcement. A second actuator applied a constant axial load $N=150$ kN on the
136 column (see Fig. 2), which corresponds to an approximate axial load ratio $v=N/(f_{cm}A_g)=0.07$, where A_g is the
137 column gross cross sectional area. The formation and development of cracks were monitored continuously
138 during the test. Moreover, the tests were paused at the onset of the first visible diagonal core cracking (which
139 appeared suddenly) to record the applied load and tip displacement. The tests were halted when the load
140 capacity of the joints dropped to approximately 50% of the peak load.

141 **CFRP strengthening**

142 Fig. 3(a) shows a general view of the CFRP strengthening sequence. The main goal of the strengthening was
143 to develop the plastic capacity of the beam reinforcement. To achieve this, the premature failure of the core
144 zone had to be prevented and the flexural capacity of the column enhanced.

145 **Strengthening of joint core**

146 The CFRP strengthening was designed considering the total shear capacity of the joint core as the sum of
147 concrete and CFRP contributions. The concrete contribution (V_c) was computed according to ASCE/SEI 41-

148 06 (2007) using Eq. (1), a shear strength coefficient $\gamma=0.083 \times 6 \sqrt{\text{psi}}=0.50 \sqrt{\text{MPa}}$ and the strength of the new
 149 concrete core (see Table 1).

$$V_c = \gamma A_j \sqrt{f_c} = (0.5)(260)(260)\sqrt{55} = 250 \text{ kN} \quad (1)$$

150 where A_j is the effective horizontal joint area.

151 The theoretical shear force required to develop the plastic capacity of the beam reinforcement V_{jh} (associated
 152 to a beam load $P_y=\pm 106 \text{ kN}$) was computed using force equilibrium according to Eq. (2).

$$V_{jh} = T_b - V_{col} = P \left[\frac{L_b}{z} - \frac{L_b + 0.5h_c}{H_c} \right] = 106000 \cdot \left[\frac{1370}{0.875(362)} - \frac{1370 + 0.5(260)}{2400} \right] = 392 \text{ kN} \quad (2)$$

153 where T_b is the tension force of the top beam reinforcement; V_{col} is the column shear; L_b is the beam length to
 154 the applied load point; H_c is the distance between column supports; h_c is the height of the column cross
 155 section; and z is the lever arm of the beam flexural moment (assumed equal to 0.875 the beam effective
 156 depth).

157 Thus, the shear to be resisted by the CFRP sheets is $V_f=392-250=142 \text{ kN}$. The required number of CFRP
 158 layers was determined using ACI 440.2R-08 guidelines (ACI Committee 440 2008) adopting the
 159 recommended value of effective CFRP strain ($\epsilon_{fe}=0.004$) and $\alpha=90^\circ$:

$$n = \frac{V_f}{2t_f \epsilon_{fe} E_f d_{fv}} = \frac{142000}{2(0.185)(0.004)(241000)(222)} = 1.6 \text{ layers} \Rightarrow 2 \text{ layers} \quad (3)$$

160 where d_{fv} is the effective depth of FRP shear reinforcement.

161 Accordingly, a minimum of two layers of CFRP were required to strengthen the joint core. As shown in Fig.
 162 3(a), U-shaped CFRP sheets strengthened the joint core to increase its shear strength (layer ①). Confining
 163 sheets (layer ②) were then wrapped around the beam to prevent premature debonding of the U-shaped
 164 sheets.

165 **Strengthening of column**

166 The flexural capacity of the column was increased by bonding CFRP sheets parallel to the column axis
167 (layers ③ and ④ in Fig. 3(a)). The number of layers required to satisfy a hierarchy strength
168 $\Sigma M_{Rcol} > 1.3 \Sigma M_{Rbeam}$ was determined using conventional moment-curvature analysis assuming perfect bond
169 between CFRP sheets and concrete. The presence of the beam hindered the continuity of sheets ③ on the
170 inner part of the column. To avoid interrupting or mechanically anchoring sheets ③ in the beam section,
171 these sheets were folded and bonded on the column faces. As a result, sheets ③ provided slightly lower
172 flexural strength in comparison to sheets ④. Nonetheless, detailed moment-curvature analyses indicate that
173 such difference is less than 10%, which is acceptable for practical strengthening applications. An additional
174 layer of CFRP (⑤) was bonded on both sides of the column to keep sheets ③ in place during the subsequent
175 installation of the confining sheets. Finally, sheets ⑥ and ⑦ were used to increase the ductility of the
176 column and to avoid premature debonding of ③, ④ and ⑤.

177 Table 2 summarizes the number of CFRP sheets used for each joint. In joint JA2RF, sheets ① had a shorter
178 bonded length to examine its effect on the resulting confinement level of the joint core and overall joint
179 behavior. As shown later, the relatively low capacity of joint JA2RF showed that two layers of CFRP sheets
180 ① were insufficient to develop the plastic capacity of the beam reinforcement. Therefore, three CFRP layers
181 were used for joints JB2RF and JC2RF (Table 2). Also, two layers of confining sheets ②, ⑥ and ⑦ were
182 used in the latter joints as one layer did not prevent premature fiber debonding at beam and column corners of
183 joint JA2RF. No mechanical anchors or steel plates were utilized to prevent debonding of CFRP sheets.

184 After the tests on joint JB2RF, the CFRP sheets were completely removed and the core was replaced again
185 following the same procedure described previously (see Fig. 3(b)). Post-tensioned steel strapping was applied
186 to the beam and column outside the core to promote the development of shear cracks in the core, and the joint
187 was retested (JB2R).

188 It should be noted that in actual rehabilitation of damaged buildings, the removal and recast of the concrete
189 core would require the use of temporary shoring adjacent to the joint. Shoring can be removed after the recast

190 core sets, thus allowing the preparation of concrete surfaces for the application of CFRP sheets. In real CFRP
191 strengthening applications adopting the layout shown in Fig. 3(a), sheets ③ could be bonded (completely
192 unfolded) on the inner face of the column, and then secured using mechanical CFRP anchors embedded in the
193 concrete. Such anchoring solution was proven effective at preventing debonding of the CFRP strengthening
194 on a substandard full-scale RC building tested by the authors (Garcia et al. 2010).

195 **Test results and discussion**

196 Table 3 reports a) the load and drift ratio at the onset of diagonal cracking in the core (P_{cr} and δ_{cr} ,
197 respectively), b) the load and drift ratio at peak load (P_{max} and δ_{max} , respectively), c) enhancement in peak
198 load (ΔP_{max}) over the bare specimens, and d) ultimate drift ratio (δ_u) causing a 50% drop in P_{max} . The results
199 are presented for the push (+) and pull (-) directions. The following sections summarize the most significant
200 observations of the testing program and discuss the results shown in Table 3.

201 ***Bare and rehabilitated joints***

202 The progression of damage and final failure mode of the bare and rehabilitated joints were very similar.
203 Despite the short anchorage length of the bottom beam reinforcement, pull out failure was not observed. This
204 was confirmed by experimental observations (no cracks formed at the beam-joint interface) and by
205 comparison of readings from strain gages fixed on the bars with displacements. Narrow splitting cracks
206 formed along the spliced reinforcement in the column. As shown in Fig. 4(a) and (b), final failure of the bare
207 and rehabilitated specimens was dominated by extensive diagonal cracking and partial concrete spalling in
208 the core zone (J-type failure).

209 The load-drift responses of the bare joints (Fig. 5(a)-(c)) show that the specimens remained elastic until the
210 onset of diagonal core cracking, when the load dropped slightly. Despite the lack of steel stirrups, the bare
211 specimens failed gradually and sustained drifts of up to $\pm 4.0\%$ (JC2 in Table 3). Such gradual failure is
212 attributed to progressive crushing of the diagonal concrete strut in the joint core. As shown in Table 3, the
213 load and drift at the onset of diagonal cracking were similar for all bare joints, regardless of the type of
214 detailing in the beam reinforcement. The peak load for all bare joints was achieved at very similar $\delta_{max} \pm 1.4-$

215 1.5% in both the push and pull directions and no pullout failure occurred during the tests because shear
216 failure dominated the response. The lower loads resisted in the pull direction (Table 3) can be due to damage
217 produced by the cyclic loading regime. The influence of the different anchorage solutions used for the joints
218 was examined in another study (Jemaa 2013).

219 The load-drift relationship of joint JB2R in Fig. 5(d) shows the effect of core replacement on the shear
220 strength of the joint (see also Table 3). Compared to JB2, the rehabilitation enhanced the peak capacity of
221 joint JB2R by an average of 44%. This confirms that, in spite of severe damage produced in the joints during
222 testing phases 1 and 2, the high-strength concrete used in the core recast and the welding of the top and
223 bottom beam reinforcement (JB2R only) enhanced considerably the joint capacity. Note that although the
224 beam reinforcement did not pullout during the tests, such bars were welded in JB2R to correct excessive
225 permanent deformations and to assess the effectiveness of this strengthening solution as pullout failure was
226 not desired. This approach was also adopted in the joints of a full-scale building tested recently by the authors
227 (Garcia et al. 2014a).

228 Whilst in this study the joint specimens were tested up to a drift level of $\pm 4.0\%$ to produce severe damage and
229 help understand their vulnerability, it is evident that the residual value and capacity of an actual substandard
230 building pushed to such drift value would be relatively low. Nonetheless, concrete core replacement can be
231 carried out at lower levels of drift or damage and is justified when, for instance, the building experience
232 extensive shear damage or was cast with low-strength concrete ($f_{cm} < 20$ MPa). Poor quality concrete is a
233 common deficiency of many low-rise substandard constructions of developing countries.

234 ***CFRP-strengthened joints***

235 As the CFRP sheets were bonded directly onto the concrete surface, the onset of diagonal cracking in the
236 joint core could not be observed. No damage was observed in the CFRP sheets, but extensive “crackling”
237 noise at a drift ratio $\delta \pm 1.0\%$ indicated that debonding was taking place at different locations. In specimen
238 JA2RF, full debonding of sheets ① and the rupture of sheets ② at δ of $\pm 3.0\%$ led to premature failure of the
239 CFRP strengthening. In contrast, total rupture of sheets ① occurred across the beam depth (just above sheets

240 ③) at $\delta \pm 5.0\%$ and $\pm 4.0\%$ in joints JB2RF and JC2RF, respectively. Although no mechanical anchors were
241 used, sheet debonding did not occur in these joints. Fig. 6(a) and (b) show specimens JA2RF and JB2RF at
242 the end of the tests. The removal of the CFRP sheets after the tests revealed extensive diagonal cracking in
243 the core, but the width and extension of cracks reduced considerably in comparison to the bare specimens. No
244 evident damage was observed in the lap splices or in the columns outside the CFRP-strengthened area.
245 However, the beams of joints JB2RF and JC2RF experienced significant flexural cracking outside the CFRP-
246 strengthened region.

247 Fig. 7(a) to (c) show the load-drift relationships for the CFRP-strengthened specimens. The combination of
248 core replacement and CFRP strengthening enhanced significantly the load and deformation capacity of the
249 joints. Compared to the bare counterparts, the peak load of specimens JA2RF, JB2RF and JC2RF increased
250 by an average of 52%, 145% and 128%, respectively (see Table 3). Moreover, the peak and ultimate drift
251 ratios of the joints also increased by up to 97% and 67%, respectively (joint JB2RF). Fig. 7(a) to (c) show
252 that the area enclosed by the hysteretic loops is significantly larger for the CFRP-strengthened joints than for
253 the bare specimens, which implies that these joint had a higher energy dissipation capacity.

254 Fig. 8 shows envelopes of the load-drift ratio relationships of the tested joints. The results indicate that the
255 bare specimens resisted only 40-55% of the load required to develop the plastic capacity of the beam, P_y (see
256 also Table 3). The peak load of specimen JA2RF reached 78% of P_y as premature debonding of the CFRP
257 sheets occurred. In contrast, specimens JB2RF and JC2RF developed some yielding in the top and bottom
258 beam reinforcement as shown by short post-yield incursions in Fig. 8. Readings from strain gages also
259 confirmed that the beam reinforcement of the joints developed strains of up to 4000-5000 $\mu\epsilon$ (e.g. Fig. 9). As
260 a result, joints JB2RF and JC2RF failed in a more ductile BJ-type mode (i.e. joint failure after yielding of
261 beam reinforcement), thus achieving the strengthening goals. However, CFRP rupture and excessive damage
262 in the joint core prevented the development of larger plastic strains in the beam reinforcement.

263 **Stiffness degradation and shear stress-strain response**

264 Fig. 10 compares the stiffness degradation of the tested specimens. The secant stiffness is defined by the
265 slope of a line connecting the maximum drifts in the push and pull directions of the first hysteresis loop. The
266 results indicate that the core recast was very effective at restoring the original stiffness of the CFRP-
267 strengthened specimens. The stiffness of JB2R was not fully recovered and this can be attributed to the
268 flexural cracks formed in the beam of this joint during the previous tests (JB2 and JB2RF, see Fig. 10). In
269 comparison to the bare specimens, it is also evident that the CFRP strengthening of the joints reduced
270 significantly the rate of stiffness degradation. The fast stiffness deterioration after $\delta \pm 2.0\%$ in the CFRP-
271 strengthened specimens can be attributed to the onset of CFRP rupture and to damage in the core.

272 Fig. 11 compares the experimental shear stress-strain response of joints JC2 and JC2RF, which are
273 representative of the rest of the specimens. Shear strains were derived using average measurements of the
274 linear potentiometers located at the joint core. Results in Fig. 11 are only shown up to the point where the
275 potentiometers failed, after reaching the joint capacity. It is shown that average joint strains at peak load
276 (P_{max}) of specimens JC2 and JC2RF were 0.0067 and 0.069 rad, respectively, whereas maximum joint strains
277 were 0.025 and 0.11 rad. The considerable enhancement in joint deformation capacity of joint JC2RF is
278 attributed to the rehabilitation/strengthening intervention. Due to space limitations, the detailed analysis of
279 the joint strains will be published by the authors in a future paper.

280 **CFRP strains**

281 Typical strain readings (see Fig. 12(a)) from gages located at the core zone of the specimens indicate that, as
282 expected, CFRP strains were negligible at the beginning of the test and increased after the onset of diagonal
283 core cracking. In general, the CFRP strain values measured at peak load (P_{max}) varied from 2500 $\mu\epsilon$ (joint
284 JA2RF) to 7300 $\mu\epsilon$ (JB2RF), and at ultimate drift (δ_u) varied from 11900 $\mu\epsilon$ (JA2RF) to 16900 $\mu\epsilon$ (JB2RF).
285 The latter values correspond to 70% and 100% of the ultimate strain of the CFRP sheets, respectively. Fig.
286 12(b) shows typical strain readings from gages fixed on the confining sheets (6) at the mid-point of the lap
287 splice length (see Fig. 3(a)). Overall, maximum strains at P_{max} varied from 200 to 570 $\mu\epsilon$ only, whereas
288 strains at δ_u were always lower than 1000 $\mu\epsilon$. These results confirm previous research by the authors (Garcia

289 et al. 2013; 2014b) that showed that low CFRP strains ($\epsilon_f < 1600 \mu\epsilon$) develop in CFRP-confined lap-spliced
290 RC members dominated by bond splitting failure.

291 **Contribution of rehabilitation and CFRP to total joint shear strength**

292 The maximum capacities of the strengthened joints reported in Table 3 include the contributions of the
293 replaced core and the CFRP strengthening. To decouple the individual contribution of the replaced core, the
294 shear strength factor γ included in current guidelines (e.g. ACI-ASCE Committee 352 2002) is adopted in this
295 study. Table 4 summarizes the experimental shear stress v_{jh} (computed using Eq. (4)) and corresponding
296 factor γ for the tested joints. The reported values are the average of the push and pull directions.

$$v_{jh} = V_{jh} / A_j \quad (4)$$

297 For comparison, Table 4 also shows the factors γ ($\gamma = v_{jh} / \sqrt{f_c}$) computed using existing predictive models: γ_P
298 Priestley (1997); γ_{KL} Kim and LaFave (2009); γ_{HJ} Hassan (2011) for J-type failure; γ_{HS} Hassan (2011) for S-
299 type failure due to the pullout of the straight bottom beam reinforcement; and γ_{PM} Park and Mosalam (2012).
300 A “virtual” joint index of 0.0139 was adopted to determine γ_{KL} for joints without shear reinforcement as
301 suggested by Kim and LaFave (2009). Table 4 also includes the shear strength factor γ_{A41} for exterior joints
302 given by the ASCE/SEI 41-06 (2007) guidelines.

303 Table 4 shows that the bare specimens have similar shear strength factors γ ranging from 0.49 to 0.52.
304 Moreover, despite the damage produced during testing phases 1 and 2, specimen JB2R had a similar factor
305 $\gamma = 0.53$. This indicates that the replaced core resisted a shear stress comparable to that of the bare joints. It is
306 shown that the approaches proposed by Priestley, Kim and LaFave, Hassan for J-type failure and Park and
307 Mosalam overestimate the experimental shear strength factors γ by an average of 13%, 77%, 48% and 85%,
308 respectively. Conversely, Hassan’s S-failure model always underestimates γ by an average of 44%. This
309 underestimation may be due to the calibration of the model, which was done using joints with short
310 anchorage lengths of 152 mm only. Whilst recent research (e.g. Park and Mosalam 2013) suggests that ASCE
311 41 may yield conservative estimates for the shear strength of substandard joints, it predicted accurately the

312 values γ of the bare and rehabilitated joints tested in this research. Consequently, ASCE 41 is used in this
313 study to evaluate the shear strength of the recast cores.

314 Table 4 also shows the decoupled contributions of the recast core and CFRP strengthening for the CFRP-
315 strengthened specimens. In this table, $v_{jh,core}$ and $v_{jh,CFRP}$ are the shear stress contributions of the recast core
316 and CFRP strengthening to the total joint capacity, respectively; and $\Delta v_{jh,core}$ and $\Delta v_{jh,CFRP}$ are the
317 corresponding shear stress enhancements. For specimen JB2RF, $v_{jh,core}$ was taken as the shear stress of the
318 corresponding rehabilitated specimen JB2R. For joints JA2RF and JC2RF, $v_{jh,core}$ was computed adopting
319 $\gamma=0.50\sqrt{\text{MPa}}$ and the concrete strength of the replaced core listed in Table 1. The value $v_{jh,CFRP}$ was then
320 calculated as the difference between the experimental shear stress v_{jh} of the CFRP-strengthened joints and
321 $v_{jh,core}$. The rehabilitation and strengthening were very effective at increasing the shear strength of the joints,
322 with the new core contributing by up to 44% of the total and the externally bonded CFRP by up to 69% (see
323 joints JB2RF and JC2RF in Table 4). It should be mentioned that the experimental shear strength factors
324 obtained for joints JB2RF and JC2RF ($\gamma=0.85\sqrt{\text{MPa}}$ and $0.83\sqrt{\text{MPa}}$, respectively) are only 15 and 17% lower
325 than the factor $\gamma=1.0\sqrt{\text{MPa}}$ considered in ACI 352R-02 (2002) for the design of code-compliant exterior
326 joints. As the capacity of the joints is not expected to increase significantly after yielding of the beam
327 reinforcement, the experimental factors γ reported here are considered as maximum achievable values. This
328 implies that the amount of CFRP utilized in the strengthening was sufficient to develop the full available
329 plastic capacity of the joints.

330 **Summary and conclusions**

331 This paper presented test results of three substandard full-scale RC beam-column joints subjected to two
332 successive testing phases. The geometry and detailing of the specimens were similar to those used in a full-
333 scale substandard RC building tested on a shake table as part of BANDIT Project (Garcia et al. 2014a). In
334 phase 1, the bare joints were subjected to cyclic tests up to a load that induced a 50% drop in peak capacity.
335 As these tests produced severe damage in the joint core, the damaged concrete was fully removed and
336 replaced with new high-strength concrete. The specimens were subsequently strengthened with externally

337 bonded CFRP sheets and retested up to failure in phase 2. From the test results and analysis presented here,
338 the following conclusions can be drawn:

339 1) The behavior of the bare joints was dominated by extensive cracking in the concrete core which led to
340 premature shear failure (J-type failure). The capacity of the bare specimens was approximately 40-55% the
341 plastic capacity of the joints. Despite the substandard anchorage used for the bottom beam reinforcement, no
342 pullout failure occurred during the tests.

343 2) The final failure mode of the rehabilitated joint JB2R was similar to that observed in the bare counterparts
344 (J-type). However, the complete core replacement using high-strength concrete restored the original stiffness
345 of the severely damaged joints and increased their capacity by up to 44%.

346 3) The CFRP strengthening enhanced the capacity of the joints by up to 145% over the bare counterparts
347 (joint JB2RF), and by up to 69% over the specimens rehabilitated with a new core (JB2RF and JC2RF).
348 Compared to the bare joints, the ultimate drift of the CFRP-strengthened joints was enhanced by up to 66%
349 (JB2RF). The use of CFRP strengthening also resulted in yielding of the beam reinforcement and led to a
350 more ductile BJ-type of failure. Although the adopted strengthening layout prevented sheet debonding
351 without the use of mechanical anchors, CFRP rupture and excessive damage in the joint core prevented the
352 development of large plastic strains in the beam reinforcement.

353 4) For the bare and rehabilitated joints presented here, the approaches proposed by Priestley (1997), Kim and
354 LaFave (2009), Hassan (2011) for J-type failure and Park and Mosalam (2012) overestimate the experimental
355 shear strength factors γ by an average of 13%, 77%, 48% and 85%, respectively. Conversely, Hassan's model
356 for S-type failure underestimates γ by an average of 44%. The shear strength factor $\gamma=0.50\sqrt{\text{MPa}}$ given by
357 ASCE/SEI 41-06 (2007) for exterior joints predicts the shear strength of the bare and rehabilitated joints with
358 very good accuracy.

359 5) The amount of CFRP utilized in the strengthening was sufficient to develop the full plastic capacity of the
360 joints. The experimental shear factors γ of joints JB2RF and JC2RF ($\gamma=0.85\sqrt{\text{MPa}}$ and $0.83\sqrt{\text{MPa}}$,

361 respectively) are only 15 and 17% lower than that considered in ACI 352R-02 (2002) for the design of code-
362 compliant exterior joints ($\gamma=1.0\sqrt{\text{MPa}}$). Therefore, the rehabilitation/strengthening method proposed in this
363 study is very effective for post-earthquake strengthening of typical substandard structures of developing
364 countries.

365 **Acknowledgements** R. Garcia thankfully acknowledges the financial support provided by CONACYT and DGRI-SEP (Mexico). Y.
366 Jemaa and Y. Helal thankfully acknowledge the financial support provided by Al-Baath University and Damascus University (Syria),
367 respectively. The CFRP system (Tyfo SCH-41.5X) was kindly provided by Fyfe Europe S.A.

368 References

- 369 ACI Committee 440 (2008). "ACI 440.2R-08 Guide for the Design and Construction of Externally Bonded FRP
370 Systems for Strengthening Concrete Structures." American Concrete Institute, Farmington Hills, MI.
- 371 ACI-ASCE Committee 352 (2002). "ACI 352R-02 (Reapproved 2010) Recommendations for Design of Beam-Column
372 Connections in Monolithic Reinforced Concrete Structures." Joint ACI-ASCE Committee 352, Farmington Hills, MI.
- 373 Akguzel, U., and Pampanin, S. (2010). "Effects of variation of axial load and bi-directional loading on seismic
374 performance of GFRP retrofitted reinforced concrete exterior beam-column joints." *J. Compos. Constr.*, 14(1), 94-104.
- 375 Al-Salloum, Y.A., Almusallam, T.H., Alsayed, S.H., and Siddiqui, N.A. (2011). "Seismic behavior of as-built, ACI-
376 complying, and CFRP repaired exterior RC beam-column joints." *J. Compos. Constr.*, 15(4), 522-534.
- 377 Al-Salloum, Y.A., Siddiqui, N.A., Elsanadedy, H.M., and Abadeland, A.A. (2011). "Textile-Reinforced Mortar versus
378 FRP as strengthening material for seismically deficient RC beam-column Joints." *J. Compos. Constr.*, 15(6), 920-933.
- 379 Alsayed, S.H., Al-Salloum, Y.A., Almusallam, T.H., and Siddiqui, N.A. (2010). "Seismic response of FRP-upgraded
380 exterior RC beam-column joints", *J. Compos. Constr.*, 14(2), 195-208.
- 381 Antonopoulos, C.P., and Triantafillou, T.C. (2003) "Experimental investigation of FRP-strengthened RC beam-column
382 joints." *J. Compos. Constr.*, 7(1), 39-49.
- 383 ASCE/SEI 41-06 (2007). "Seismic Rehabilitation of Existing Buildings." American Society of Civil Engineers, Reston,
384 VA.
- 385 Bousselham, A. (2010). "State of research on seismic retrofit of RC beam-column joints with externally bonded FRP." *J.*
386 *Compos. Constr.*, 14(1), 49-61.
- 387 BSI (2009a) "BS EN 12390-3:2009 - Testing hardened concrete Part 3: Compressive strength of test specimens." British
388 Standards Institution, London, UK.
- 389 BSI (2009b) "BS EN 12390-6:2009 - Testing hardened concrete Part 6: Tensile splitting strength of test specimens."
390 British Standards Institution, London, UK.
- 391 El-Amoury, T., and Ghobarah, A. (2002). "Seismic rehabilitation of beam-column joint using GFRP sheets." *Eng.*
392 *Struct.*, 24(11), 1397-1407.
- 393 Garcia R, Hajirasouliha I, Pilakoutas K (2010) "Seismic behaviour of deficient RC frames strengthened with CFRP
394 composites." *Eng. Struct.*, 32(10), 3075-3085.
- 395 Garcia, R. (2013). "Seismic strengthening of substandard RC structures using external reinforcement." PhD Thesis, The
396 Univ. of Sheffield, Sheffield, UK.
- 397 Garcia, R., Hajirasouliha, I., Guadagnini, M., Helal, Y., Jemaa, Y., Pilakoutas, K., Mongabure, P., Chrysostomou, C.,
398 Kyriakides, N., Ilki, A., Budescu, M., Taranu, N., Ciupala, M.A., Torres, L., Saiidi, M. (2014a). "Full-scale shaking
399 table tests on a substandard RC building repaired and strengthened with Post-Tensioned Metal Straps". *J. Earthq. Eng.*,
400 18(2).

401 Garcia, R., Helal, Y., Pilakoutas, K., and Guadagnini, M. (2013). "Bond strength of short splices in RC beams confined
402 with steel stirrups or external CFRP." *Mater. Struct.* DOI: 10.1617/s11527-013-0183-5, in press.

403 Garcia, R., Helal, Y., Pilakoutas, K., and Guadagnini, M. (2014b). "Bond strength of substandard laps in RC beams
404 confined with externally bonded CFRP." *Constr. Build. Mater.* 50(15 January), 340-351.

405 Gdoutos, A., Pilakoutas, K., and Rodopoulos, C. (2000). "Failure analysis of industrial composite materials." McGraw-
406 Hill Companies, NY, 51-108.

407 Gergely, J., Pantelides, C.P., and Reaveley, L.D. (2000). "Shear strengthening of RCT-joints using FRP composites." *J.*
408 *Compos. Constr.*, 4(4), 198-205.

409 Ghobarah, A., and El-Amoury, T. (2005). "Seismic rehabilitation of deficient exterior concrete frame joints." *J. Compos.*
410 *Constr.*, 9(5), 408-416.

411 Ghobarah, A., and Said, A. (2001). "Seismic rehabilitation of beam-column joints using FRP laminates." *J. Earthq.*
412 *Eng.*, 5(1), 113-129.

413 Ghobarah, A., and Said, A. (2002). "Shear strengthening of beam-column joints." *Eng. Struct.*, 24(7), 881-888.

414 Granata, P.J., and Parvin, A. (2001). "An experimental study on Kevlar strengthening of beam-column connections."
415 *Comp. Struct.*, 53(2), 163-171.

416 Hassan, W.M. (2011). "Analytical and Experimental Assessment of Seismic Vulnerability of Beam-Column Joints
417 without Transverse Reinforcement in Concrete Buildings." PhD Thesis, Univ. of California, Berkeley, CA.

418 Ilki, A., Bedirhanoglu, I., and Kumbasar, N. (2011). "Behavior of FRP-retrofitted joints built with plain bars and low-
419 strength concrete." *J. Compos. Constr.*, 15(3), 312-326.

420 Jemaa, Y. (2013) "Seismic behaviour of deficient exterior RC beam-column joints." PhD Thesis, The Univ. of Sheffield,
421 Sheffield, UK.

422 Karayannis, C., and Sirkelis, G. (2008). "Strengthening and rehabilitation of RC beam-column joints using carbon-FRP
423 jacketing and epoxy resin injection." *Earthq. Eng. Struct. Dyn.*, 37(5), 769-790.

424 Karayannis, C.G.; Chalioris, C.E., and Sideris, K.K (1998). "Effectiveness of RC beam-column connection repair using
425 epoxy resin injections," *J. Earthq. Eng.*, 2(2), 217-240.

426 Kim, J., and LaFave, J.M. (2009). "Joint Shear Behavior of Reinforced Concrete Beam-Column Connections subjected
427 to Seismic Lateral Loading." Report No. NSEL-020. Univ. of Illinois at Urbana-Champaign, IL.

428 Le-Trung, K., Lee, K., Lee, J., and Sungwoo, W. (2010). "Experimental study of RC beam-column joints strengthened
429 using CFRP composites." *Comp. Part B Eng.*, 41(1), 76-85.

430 Mosallam, A.S (2000). "Strength and ductility of reinforced concrete moment frame connections strengthened with
431 quasi-isotropic laminates." *Composites Part B: Engineering*, 31(6-7), 481-497.

432 Mukherjee, A., and Joshi, M. (2005). "FRPC reinforced concrete beam-column joints under cyclic excitation." *Comp.*
433 *Struct.*, 70(2), 185-199.

434 Pantelides, C., Okahashi, Y., and Reaveley, L. (2008). "Seismic rehabilitation of reinforced concrete frame interior
435 beam-column joints with FRP composites." *J. Compos. Constr.*, 12(4), 435-445.

436 Park, S., and Mosalam, K.M. (2012). "Parameters for shear strength prediction of exterior beam-column joints without
437 transverse reinforcement." *Eng. Struct.*, 36(-), 198-209.

438 Park, S., and Mosalam, K.M. (2013). "Experimental investigation of nonductile RC corner beam-column joints with
439 floor slabs." *J. Struct. Eng.-ASCE*, 139(1), 1-14.

440 Parvin, A., Altay, S., Yalcin, C., and Kaya, O. (2010). "CFRP rehabilitation of concrete frame joints with inadequate
441 shear and anchorage details." *J. Compos. Constr.*, 14(1), 72-82.

442 Priestley, M.J.N. (1997). "Displacement-based seismic assessment of reinforced concrete buildings." *J. Earthq. Eng.*,
443 1(1), 157-192.

444 Prota, A., Nanni, A., Manfredi, G., and Cosenza, E. (2004). "Selective upgrade of underdesigned reinforced concrete
445 beam-column joints using carbon fiber-reinforced polymers." *ACI Struct. J.*, 101(5), 699-707.

- 446 Said, A.M., and Nehdi, N.L. (2004). "Use of FRP for RC frames in seismic zones: Part I. Evaluation of FRP beam-
447 column joint rehabilitation techniques." *Appl. Compos. Mater.*, 11(4), 205-226.
- 448 Sasmal, S., Ramanjaneyulu, K., Novák, B., Srinivas, V., Kumar, K.S., Korkowski, C., Roehm, C., Lakshmanan, N.,
449 Nagesh, R.I. (2011). "Seismic retrofitting of nonductile beam-column sub-assembly using FRP wrapping and steel
450 plate jacketing." *Constr. Build. Mater.*, 25(1), 175-182.
- 451 Sezen, H. (2012). "Repair and strengthening of reinforced concrete beam-column joints with fiber-reinforced polymer
452 composites." *J. Compos. Constr.*, 16(5), 499-506.
- 453 Tsonos, A.G. (2008). "Effectiveness of CFRP-jackets and RC-jackets in post-earthquake and pre-earthquake retrofitting
454 of beam-column subassemblages." *Eng. Struct.*, 30(3), 777-793.
- 455 Engindeniz, M., Kahn, L.F., and Zureick, A.H. (2008). "Performance of an RC corner beam-column joint severely
456 damaged under bidirectional loading and rehabilitated with FRP composites." In: *Seismic Strengthening of Concrete
457 Buildings Using Fiber Reinforced Polymer Composites*, T. Alkhrdahi and P. Silva, eds. ACI SP258-2.

Tables

Table 1. Characteristics of beam-column joints

Phase	ID	f_{cm} (MPa)	f_{cm} (MPa)	Test condition
1	JA2	32.0(1.61)	2.44(0.16)	Original joint
	JB2	31.3(1.20)	2.41(0.21)	Original joint
	JC2	32.0(1.61)	2.44(0.16)	Original joint
2	JA2RF	54.2(3.00)	3.67(0.17)	JA2 with new recast core and CFRP
	JB2RF	55.3(1.90)	3.91(0.18)	JB2 with new recast core and CFRP
	JC2RF	56.9(1.20)	3.61(0.19)	JC2 with new recast core and CFRP
	JB2R	53.7(3.60)	3.70(0.21)	JB2RF with new recast core

Note: standard deviations shown in parenthesis

Table 2. Number of CFRP layers used for strengthening

Sheet no.	No. of CFRP layers		
	JA2RF	JB2RF	JC2RF
①	2	3	3
②	1	2	2
③	2	2	2
④	2	2	2
⑤	2	2	2
⑥	1	2	2
⑦	1	2	2

Table 3. Load and drift ratio results of tested joints

ID	P_{cr} (kN)	δ_{cr} (%)	P_{max} (kN)	δ_{max} (%)	ΔP_{max} (%)	$\delta_u^{(a)}$ (%)
JA2	+39.8	+0.47	+57.0	+1.42	-	±3.0
	-37.6	-0.50	-51.9	-1.48	-	
JB2	+42.0	+0.59	+58.0	+1.51	-	±3.0
	-43.1	-0.62	-43.3	-1.46	-	
JC2	+41.4	+0.52	+54.5	+1.40	-	±4.0
	-35.3	-0.39	-48.5	-1.49	-	
JA2RF	+49.0	+0.56	+86.2	+1.86	+51	±4.0
	-47.9	-0.54	-79.8	-2.00	+54	
JB2RF ^(b)	+63.9	+0.90	+120.0	+2.92	+107	±5.0
	-62.8	-0.87	-127.0	-2.95	+193	
JC2RF	+65.5	+0.80	+119.4	+2.91	+119	±5.0
	-53.3	-0.58	-115.0	-2.75	+137	
JB2R ^(b)	+56.7	+1.19	+75.0	+1.95	+29	±4.0
	-46.7	-1.01	-71.3	-2.87	+65	

^(a) Ultimate drift ratio applied in the test

^(b) The bottom beam bars were welded to the top beam bars

Table 4. Joint shear strength contributions of core rehabilitation and CFRP strengthening

Phase	ID	v_{jh} (MPa)	γ	γ_p	γ_{KL}	γ_{HL}	γ_{HS}	γ_{PM}	γ_{AAI}	$v_{jh,core}$ (MPa)	$v_{jh,CFRP}$ (MPa)	$\Delta D_{jh,core}$ (%)	$\Delta D_{jh,CFRP}$ (%)
1	JA2	2.96	0.52	0.58	0.90	0.75	0.28	0.99	0.50	-	-	-	-
	JB2	2.75	0.49	0.59	0.90	0.75	0.29	1.01	0.50	-	-	-	-
	JC2	2.80	0.49	0.58	0.90	0.75	NA ^(a)	0.99	0.50	-	-	-	-
2	JB2R	3.97	0.53	0.55	0.90	0.75	NA ^(a)	0.77	0.50	-	-	-	-
	JA2RF	4.51	0.61	-	-	-	-	-	0.50 ^(b)	3.68	0.83	+24	+23
	JB2RF	6.71	0.90	-	-	-	-	-	-	3.97	2.74	+44	+69
	JC2RF	6.36	0.84	-	-	-	-	-	0.50 ^(b)	3.77	2.59	+35	+69

^(a) Not applicable because the bottom beam bars cannot pullout from the core

^(b) Theoretical values based on ASCE/SEI 41-06 (2007)

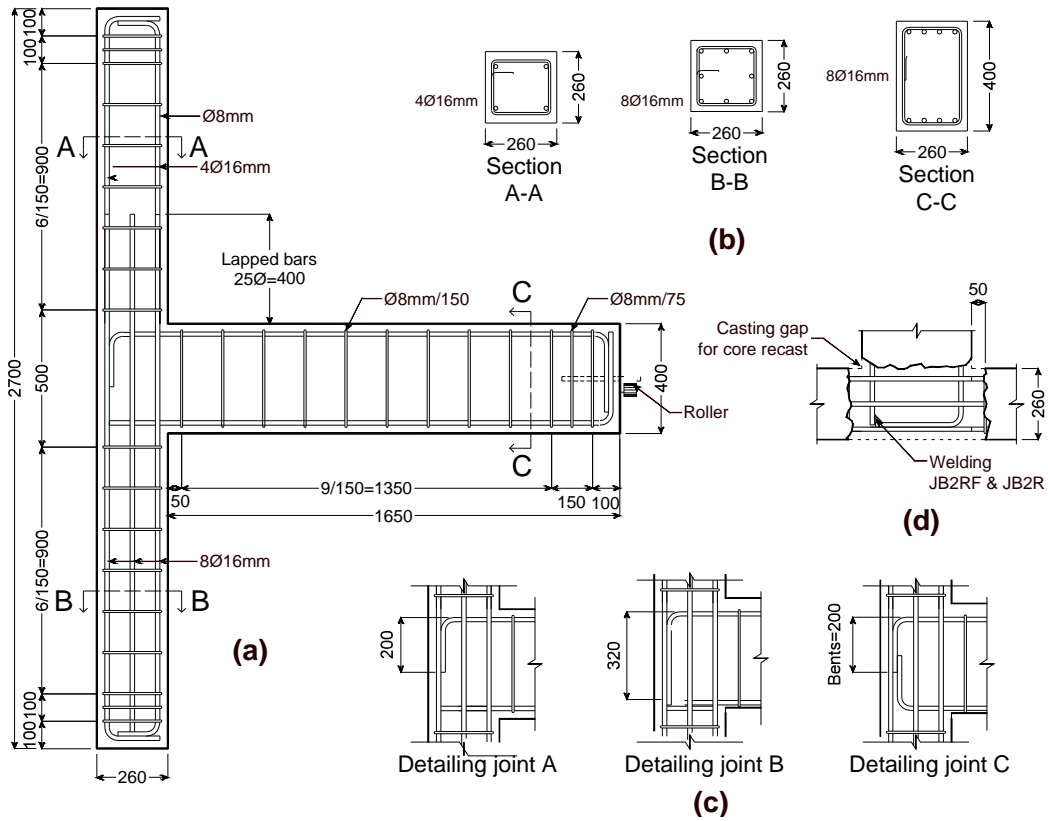


Fig. 1. General geometry and reinforcement details of tested joints (units: mm)

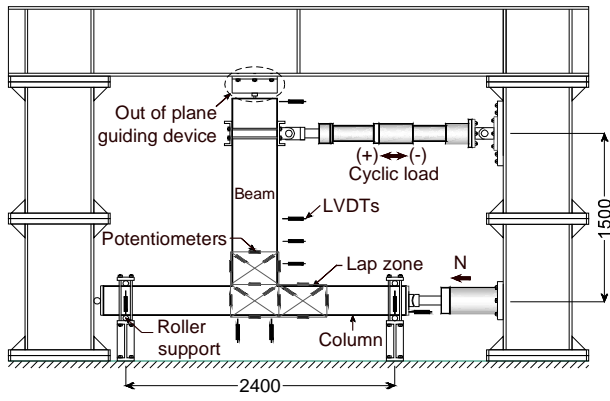


Fig. 2. Test setup and instrumentation of joints (units: mm)

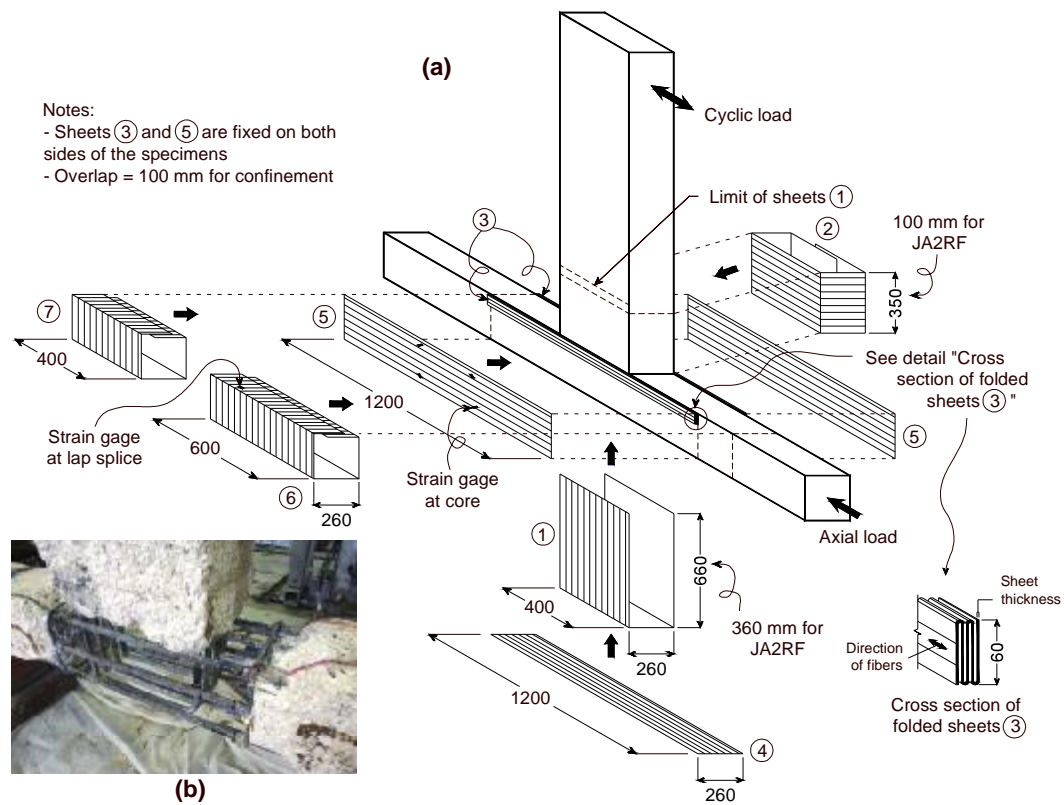


Fig. 3. (a) CFRP strengthening strategy, and (b) removal of CFRP and core replacement in joint JB2RF (units: mm)

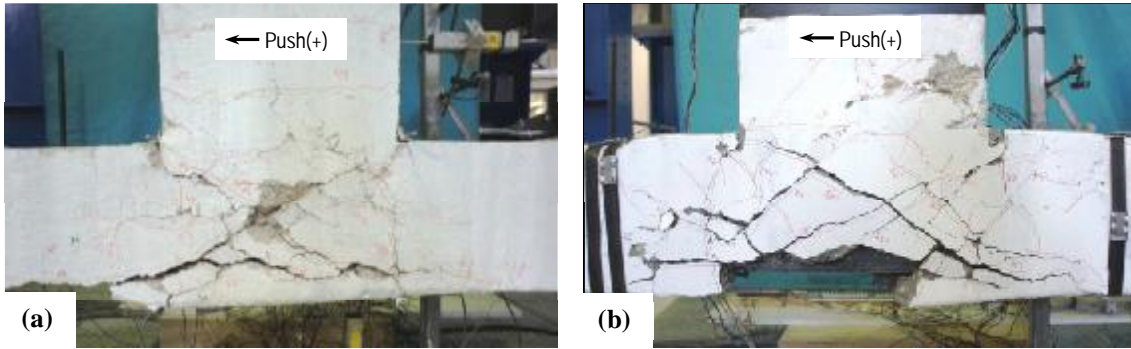


Fig. 4. Typical failure of (a) bare joints (JB2), and (b) rehabilitated joint JB2R

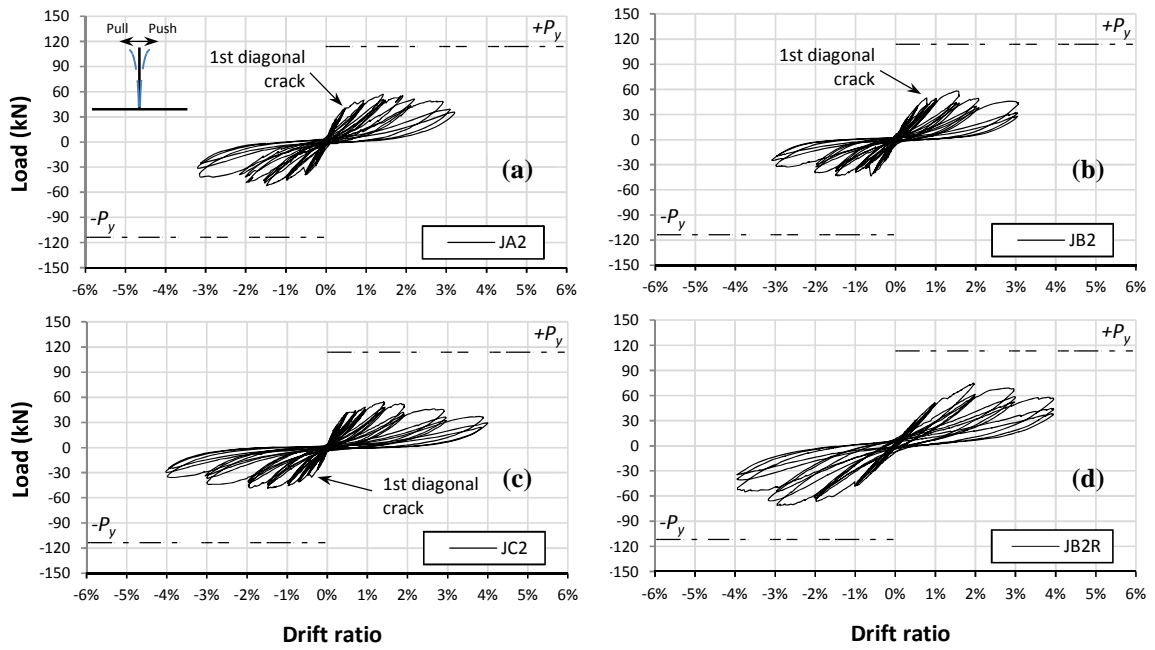


Fig. 5. Load-drift response for (a)-(c) bare joints, and (d) rehabilitated joint JB2R

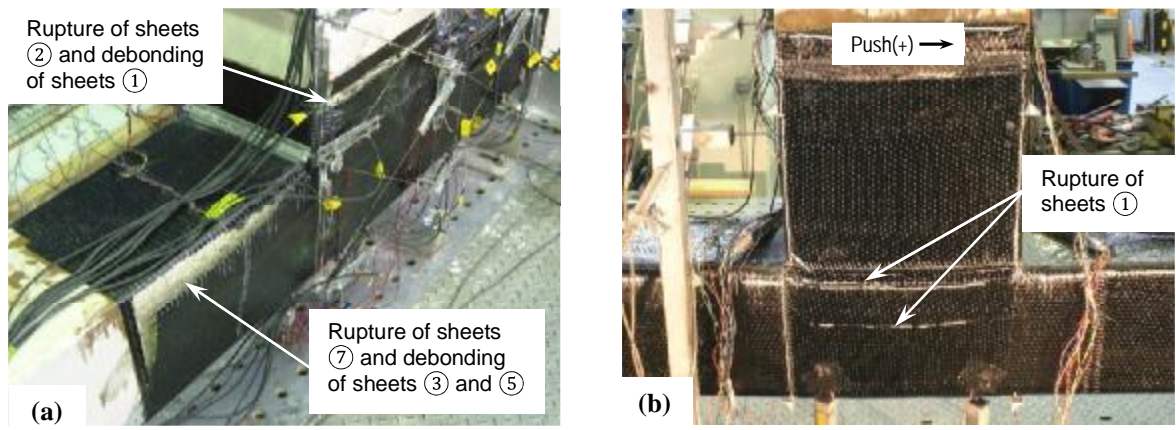


Fig. 6. Failure mode of specimens (a) JA2RF, and (b) JB2RF

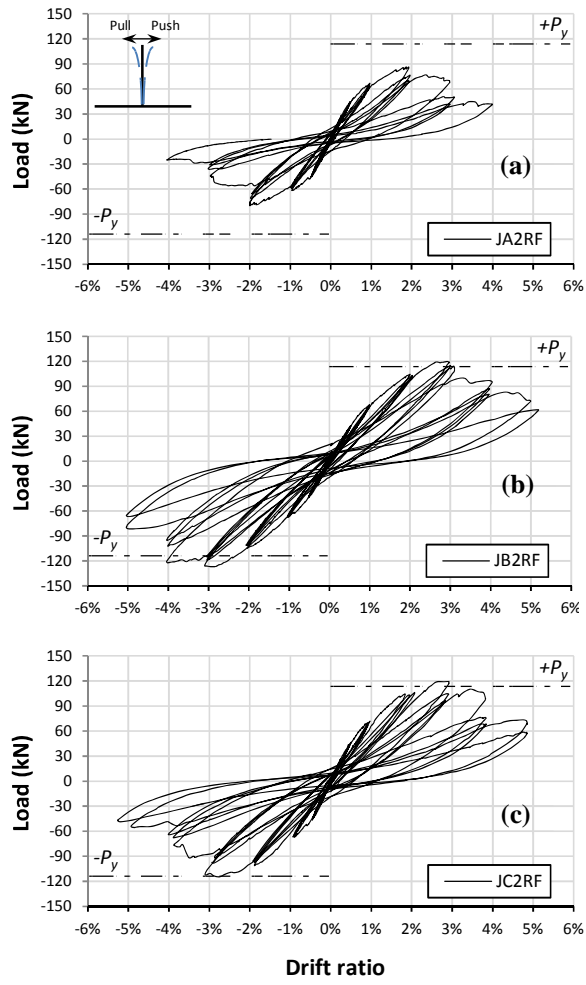


Fig. 7. Load-drift response for rehabilitated and CFRP-strengthened joints

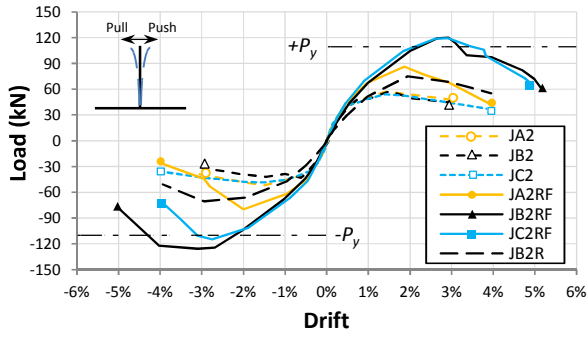


Fig. 8. Comparison of envelope from test results

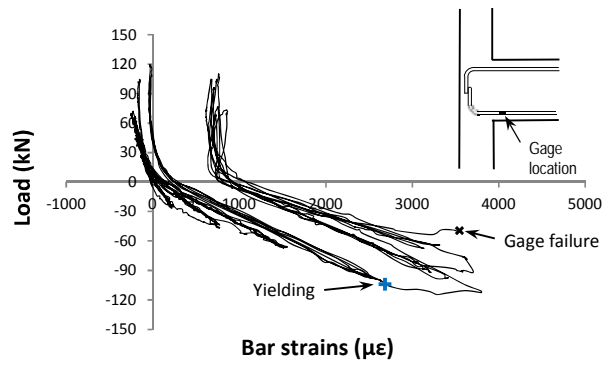


Fig. 9. Strains recorded at bottom beam reinforcement of joint JC2RF

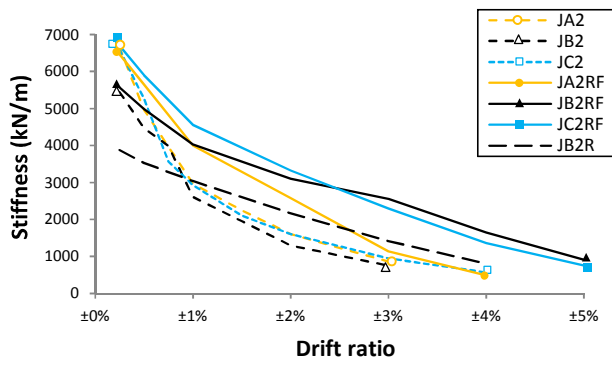


Fig. 10. Stiffness degradation of tested joints

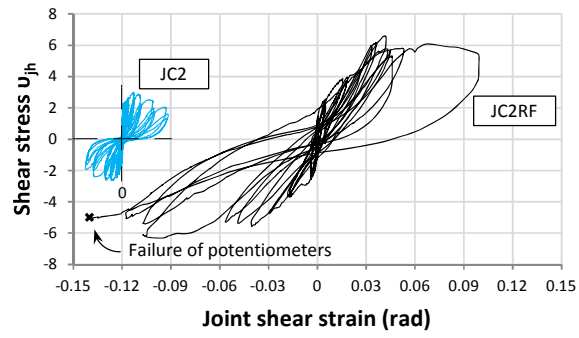


Fig. 11. Shear stress-strain of specimens (a) JC2, and (b) JC2RF

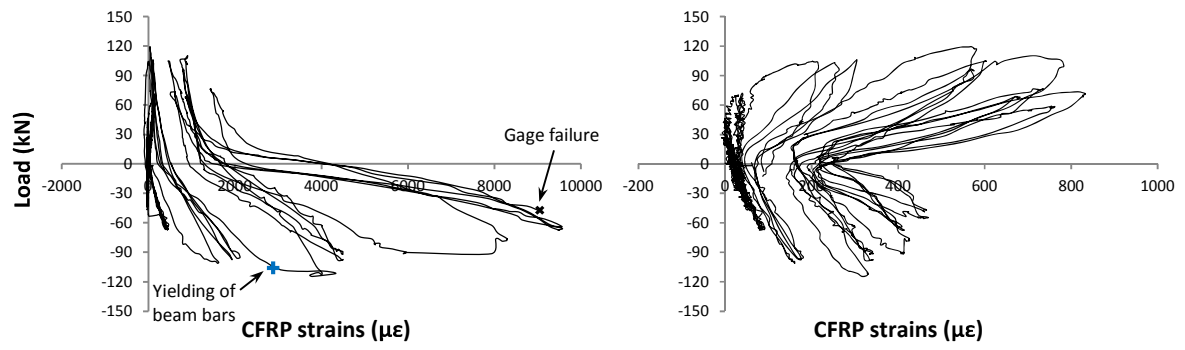


Fig. 12. Strains recorded in CFRP sheets at (a) core and (b) column lap splices of joint JC2RF